

Tunable Fano-Kondo resonance in side-coupled double quantum dot systemsChung-Hou Chung^{1,2} and Tsung-Han Lee^{1,3}¹*Electrophysics Department, National Chiao-Tung University, HsinChu, Taiwan 300, Republic of China*²*Department of Physics and Applied Physics, Yale University, New Haven, Connecticut 06520, USA*³*Department of Physics, National Tsing-Hua University, HsinChu, Taiwan 300, Republic of China*

(Received 17 May 2010; published 26 August 2010)

We study the interference between the Fano and Kondo effects in a side-coupled double quantum dot system where one of the quantum dots couples to conduction-electron bath while the other dot only side couples to the first dot via antiferromagnetic (AF) spin-exchange coupling. We apply both the perturbative renormalization-group (RG) and numerical renormalization-group (NRG) approaches to study the effect of AF coupling on the Fano line shape in the conduction leads. With particle-hole symmetry, the AF spin-exchange coupling competes with the Kondo effect and leads to a local spin-singlet ground state for arbitrary small coupling, so-called “two-stage Kondo effect.” As a result, via NRG we find the spectral properties of the Fano line shape in the tunneling density of states $\rho_c(\omega)$ of conduction-electron leads shows double dip-peak features at the energy scale around the Kondo temperature and the one much below it, corresponding to the two-stage Kondo effect; it also shows an universal scaling behavior at very low energies. We find the qualitative agreement between the NRG and the perturbative RG approaches. Relevance of our work to the experiments is discussed.

DOI: [10.1103/PhysRevB.82.085325](https://doi.org/10.1103/PhysRevB.82.085325)

PACS number(s): 72.15.Qm

I. INTRODUCTION

Fano resonance is the quantum interference effect between a localized state with finite width and a conduction band.¹ The hallmark of the Fano resonance is the asymmetric line shape in tunneling density of states (TDOS) of the conduction band. One example of Fano resonance is the transport through low-dimensional electronic (Fermi) system with local impurities. The Kondo effect² plays an important role if these impurities carry unpaired spins. Recently, there has been growing interest both theoretically and experimentally in the Fano resonance associated with the Kondo effect via the scanning tunnel microscope (STM) measurements of noble-metal surfaces^{3–9} as well as in quantum dot devices.^{10,11} The Fano resonance in these systems in general arises from two quantum interference effects: (1) between the broadened local level and the continuum conduction band and (2) between the Kondo resonance in the local level and the conduction band. The combined two effects give rise to rather complicated line shape in STM measurement of the TDOS. The Fano resonance in TDOS of conduction electrons in such systems can be served as an alternative approach to study the Kondo effect in addition to the local density of states (LDOS) of the quantum dot. The Fano line shape in TDOS of conduction electrons in the leads of a single Kondo dot system has been extensively studied, and it is sensitive to both the spatial phase of the free-conduction electrons and the scattering phase shift associated with the Kondo effect.

Very recently, the Fano resonance has been extended experimentally¹² and theoretically^{13–15} to the side-coupled double quantum dot system where the competition between Kondo and Fano effects gives rise to change in conductance profile. In this paper, we investigate the Fano-Kondo interference in the side-coupled double quantum dot systems where only one of the two dots (dot 1) connects to the leads while the other isolated dot (dot 2) is side coupled to

dot 1.^{16,17} In the Kondo limit where charging energy on each dot is large, an antiferromagnetic (AF) spin-exchange coupling is generated via the second-order hopping between two dots competes with the Kondo effect, leading to local spin-singlet ground state for arbitrary finite values of J , so-called “two-stage Kondo effect.”^{16–18} Previous studies on the side-coupled double dot systems have been mostly focused on the dip of LDOS on dot 1 upon applying the AF spin-exchange coupling. However, little is known about the feedback effect of the two-stage Kondo effect mentioned above on the TDOS of conduction electrons in the leads. In this paper, we generalize the Fano line shape in TDOS of electrons in the leads as a result of the two-stage Kondo effect in side-coupled double quantum dot system. The systematic perturbative and numerical renormalization-group (NRG) approaches are applied here in the cases both with and without particle-hole symmetries. We find as a consequence of the two-stage Kondo effect, the spectral property of the Fano line shape in TDOS of the leads develops an asymmetrical double dip/peak structure; it also shows an universal scaling behavior at very low energies. We compare our NRG results with the perturbative RG analysis.

II. MODEL HAMILTONIAN

Our starting Hamiltonian for the side-coupled double dot system is the single-impurity Anderson model for dot 1 with additional antiferromagnetic spin-exchange coupling between dot 1 and the isolated dot 2 which side coupled to it.¹⁶

$$H = \sum_{k,\alpha=L,R} \epsilon_k c_{k\alpha\sigma}^\dagger c_{k\alpha\sigma} + \sum_{\alpha=L,R} \sum_{k,\sigma} (t_\alpha c_{k\alpha\sigma}^\dagger d_{1,\sigma} + \text{H.c.}) + \sum_{i\sigma} \epsilon_{di} d_{i\sigma}^\dagger d_{i\sigma} + \sum_{i=1,2} U_i n_i^\uparrow n_i^\downarrow + JS_1 S_2, \quad (1)$$

where t_L and t_R denote the tunneling amplitudes to the left and right leads, respectively, and $c_{k\alpha\sigma}^\dagger$ creates an electron in

lead $\alpha=L,R$ with spin σ . This tunnel coupling leads to a broadening of the level on dot 1, the width of which is given by $\Gamma=\Gamma_L+\Gamma_R=2\pi(i_L^2\rho_L+i_R^2\rho_R)$, with $\rho_{L/R}$ the density of states in the leads. Here, $i=1,2$ labels the two dots and $\mathbf{S}_i=(1/2)\sum_{\sigma\sigma'}d_{i\sigma}^\dagger\sigma_{\sigma\sigma'}d_{i\sigma'}$ is their spin. Each dot is subject to a charging energy, $U_1\approx U_2=U=E_C$. In the presence of particle-hole symmetry, we have $\epsilon_{di}=-\frac{U_i}{2}$. Note that in the Kondo limit where the charging energy E_C is large, the direct hopping between the two dots are strongly suppressed and an antiferromagnetic spin-exchange coupling $J>0$ is generated via the second-order hopping processes.

The physical observables of our interest are (i) LDOS of impurity on dot 1: $\rho_{d1}(\omega)=\frac{-1}{\pi}\text{Im}G_{d1}(\omega)$ and (ii) the TDOS of the conduction electron $\rho_c(\omega)$: $\rho_c(\omega)=\rho_0+\delta\rho_c(\omega)$, where $\rho_0=\rho_{L/R}$ is the constant density of states of the bare conduction-electron leads (here we assume symmetrical leads $\rho_L=\rho_R$): $\rho_0=\frac{-1}{\pi}\text{Im}G_c^0(\omega=0)$ with $G_c^0(\omega-i\eta)$ being the bare conduction-electron Green's function, and $\delta\rho_c(\omega)$ is the correction to the LDOS of the conduction electron due to the coupling between leads and the quantum dot system: $\delta\rho_c(\omega)=\frac{-1}{\pi}\text{Im}\delta G_c(\omega-i\eta)$. Here, the correction to the conduction-electron Green's function $\delta G_c(\omega-i\eta)$ is given by

$$\delta G_c(\omega-i\eta)=\frac{\Gamma}{\pi\rho_0}G_c^0(\omega-i\eta)G_{d1}(\omega-i\eta)G_c^0(\omega-i\eta). \quad (2)$$

Using Eq. (2), we have⁴

$$\delta\rho_c(\omega)=-\Gamma\rho_0\times[(q_c^2-1)\text{Im}G_{d1}(\omega-i\eta)-2q_c\text{Re}G_{d1}(\omega-i\eta)] \quad (3)$$

with q_c being defined as

$$q_c=-\frac{\text{Re}G_c^0(\omega-i\eta)}{\text{Im}G_c^0(\omega-i\eta)} \quad (4)$$

and it can be treated approximately as a frequency-independent constant.^{3,4} Following Ref. 16, below we apply both perturbative RG and NRG approaches to calculate these quantities in the presence of particle-hole symmetry. Though the LDOS on dot 1 [or equivalently the imaginary part of the Green's function on dot 1, $\text{Im}G_{d1}(\omega)$] at finite AF spin-exchange coupling J via both RG and NRG has been computed in Ref. 16, the real part of $G_{d1}(\omega)$, $\text{Re}G_{d1}(\omega)$, which is also needed to analyze the spectral property of the Fano line shape in the TDOS of the conduction-electron leads [$\rho_c(\omega)$], has not yet been calculated by either perturbative RG or NRG approach. In the following, we provide a numerical and analytical analysis on the Fano line shape for $\rho_c(\omega)$ by analyzing both the real and the imaginary parts of $G_{d1}(\omega)$ at finite J via NRG and compare them with those via perturbative RG approach.

First, we discuss the case for $J=0$. For $J=0$ and in the presence of particle-hole symmetry ($\epsilon_{di}=-U_i/2$), it has been known that in the Kondo regime $\omega\ll T_K$ with $T_K\approx D_0e^{-\pi U_1/\Gamma}$ being the Kondo temperature for dot 1, $G_{d1}(\omega)$ is well approximated by the single Lorentzian,¹⁶

$$G_{d1}(\omega)\approx T_{d1}^0(\omega-i\eta)=\frac{z}{\omega+i\tilde{T}_K+i\eta} \quad (5)$$

with $z=c\frac{T_K}{\Gamma}$ being the quasiparticle weight at the Fermi energy, and $\tilde{T}_K=z\Gamma=cT_K$ being an energy on the order of the Kondo temperature, T_K . The precise value of the universal constant c relating T_K and \tilde{T}_K depends on the definition of T_K . Here, we define T_K as the half width of the transmission $T(\omega)\equiv-\Gamma\text{Im}G_{d1}(\omega)$. From fitting $G_{d1}(\omega)$ with the NRG data, we get $c\approx 0.5$. Note that by Fermi-liquid theory and principles of renormalization group, the AF spin-exchange interaction also gets renormalized by the same z factor: $J\rightarrow\frac{\tilde{J}}{z}$.¹⁶ Here, \tilde{J} is slightly different from J due to the large logarithmic tail in $\text{Im}G_{d1}(\omega)$. The value of \tilde{J} is obtained from the fit of $\text{Im}G_{d1}(\omega)$ to NRG data: $\tilde{J}\approx 1.1J$.¹⁶ However, for $\omega\geq T_K$, the above simple Lorentzian approximation fails to account for the large logarithmic tail in $\text{Im}G_{d1}(\omega)$. Therefore, corrections to the single Lorentzian approximation are needed in this case to more accurately describe $G_{d1}(\omega)$. Via the Dyson equation approach, taking into account the interference between the Kondo resonance and the broadened impurity level, we obtain a more accurate description for the Green's function of the dot 1 (Ref. 3)

$$G_{d1}(\omega)=G_{d1}^0(\omega)+G_{d1}^0(\omega)\tilde{T}_{d1}(\omega)G_{d1}^0(\omega), \quad (6)$$

where the bare Green's function on dot 1, $G_{d1}^0(\omega)$, describing a local impurity level with a level broadening Γ and LDOS $\rho_{d0}\equiv\frac{-1}{\pi}\text{Im}G_{d1}^0(\omega=0)$, is given by

$$G_{d1}^0=\frac{1-n/2}{\omega-\epsilon_{d1}+i\Gamma}+\frac{n/2}{\omega-\epsilon_{d1}-U_1+i\Gamma} \quad (7)$$

with $n=\langle n_{d1}^\uparrow+n_{d1}^\downarrow\rangle$ being the average occupation number on dot 1 and $\tilde{T}_{d1}(\omega)$ is the scattering T -matrix corresponding to the Kondo resonance, given approximately by³

$$\tilde{T}_{d1}(\omega-i\eta)\approx\frac{be^{i2\delta}}{\omega-\epsilon_K+i\tilde{T}_K+i\eta} \quad (8)$$

with b being a fitting parameter to be fitted with the NRG data for $\text{Im}G_{d1}(\omega)$. In the presence of particle-hole symmetry, we have $n=1$ and $\epsilon_K=0$. Here, δ in Eq. (8) corresponds to the phase shift associated with the Kondo resonance scattering, and it gives $\delta=\pi/2$ in the case of particle-hole symmetry. By fitting Eq. (6) with the NRG data, we find $b\approx z/(\pi\rho_{d0})^2$, which is in good agreement with the known result: $-\text{Im}G_{d1}(\omega=0)=1/\Gamma$ for a single impurity Anderson model.² In the Kondo regime ($\omega\ll T_K$ and $E_c\gg\Gamma$) of our system and for $J=0$, the bare Green's function on dot 1, $G_{d1}^0(\omega)$, are approximately given by $\text{Re}G_{d1}^0(\omega)\approx 0$ and $\frac{-\text{Im}G_{d1}^0(\omega)}{\pi}\approx\rho_{d0}$. The above approximations lead to the following approximated expressions for $G_{d1}(\omega)$ after including the interference between the Kondo resonance and the broadened impurity (dot 1) level via Eq. (6):

$$\text{Re}G_{d1}(\omega)\approx(\pi\rho_{d0})^2\frac{b\omega}{\omega^2+\tilde{T}_K^2}$$

$$\text{Im } G_{d1}(\omega) \approx -\pi\rho_{d0} - (\pi\rho_{d0})^2 \frac{b\tilde{T}_K}{\omega^2 + \tilde{T}_K^2} \quad (9)$$

with $\rho_{d0} = -\frac{1}{\pi} \text{Im } G_{d1}^0(\omega=0)$ being the LDOS of dot 1 at $\omega=0$. From Eqs. (3) and (9), in the Kondo limit the correction to conduction-electron density of states can therefore be expressed in terms of the well-known Fano line shape,^{3,4}

$$\delta\rho_c(\omega, J=0) \approx \rho_0 \left(\frac{q_c^2 + 2q_c\epsilon - 1}{\epsilon^2 + 1} + \beta \right), \quad (10)$$

where $\epsilon = \frac{\omega - \epsilon_K}{\tilde{T}_K}$ and $\beta = \pi\rho_{d0}\Gamma(q_c^2 - 1)$. Note that in general the Dyson equation approach in Eq. (6) is also valid for both $\omega \ll T_K$ and $\omega \approx T_K$ in the presence of large particle-hole asymmetry: $|\epsilon_{d1} - \epsilon_F| \leq \Gamma$ (with ϵ_F being the Fermi energy of the leads) where the interference between the Kondo and broadened impurity levels plays an important role in $G_{d1}(\omega)$.³

III. PERTURBATIVE RENORMALIZATION-GROUP ANALYSIS

Now, we turn on a finite AF spin-exchange coupling J . Following Ref. 16, to gain an analytical understanding we employing the perturbative renormalization-group analysis in the limit of $J \rightarrow 0$. We restrict ourselves the case with particle-hole symmetry. Though some of the aspects in this case has been studied in Ref. 16, it proves to be useful to summarize its key results for further calculations on the Fano line shape for $\rho_c(\omega)$ in the presence of AF spin-exchange coupling J . In the limit $J \rightarrow 0$, “two-stage Kondo screening” takes place.¹⁶⁻¹⁸ the spin of dot 1 first gets Kondo screened below Kondo temperature $T_K \approx D_0 e^{-\pi U_1/\Gamma}$, the first stage Kondo effect. Then for energy scale much below T_K , the second stage Kondo effect occurs at $\omega < T^* \ll T_K$ between dots 1 and 2 via the AF spin-exchange coupling J where the spin on the dot 2 gets Kondo screened. Here, the Kondo resonance peak in electron density of states on dot 1 plays the effective fermionic bath for the second stage Kondo effect. We will discuss how the Fano line shape for $\rho_c(\omega)$ is affected in the presence of the antiferromagnetic spin-exchange coupling. Summing up all leading logarithmic vertex diagrams leads to the following scaling equation for the dimensionless vertex function:¹⁶

$$\frac{d[\gamma(\omega, \tilde{T}_K)]}{dl} \equiv \frac{d[\hat{\varrho}(\omega)\tilde{J}]}{dl} = [\hat{\varrho}(\omega)\tilde{J}]^2 \quad (11)$$

with the scaling variable defined as $l \equiv \log(\tilde{T}_K/\tilde{T}'_K)$. Here, $\hat{\varrho}(\omega) \equiv \varrho(\omega)/z = \frac{1}{\pi z} \text{Im } G_{d1}(\omega)$ is the rescaled effective density of states of dot 1. Integrating this differential equation up to $l \equiv \log(\tilde{T}_K/\omega)$, one obtains the dimensionless vertex function in the leading logarithmic approximation,¹⁶

$$\gamma(\omega, \tilde{T}_K) = \frac{1}{\frac{\omega^2}{\tilde{T}_K^2} \log \frac{\tilde{T}_K}{T^*} + \log \frac{|\omega|}{T^*}} \quad (12)$$

with the second scale T^* defined as

$$T^* = \tilde{T}_K \exp(-\pi\tilde{T}_K/\tilde{J}). \quad (13)$$

The second-order self-energy correction to the retarded Green's function G_{d1}^0 simply gives the expression¹⁶

$$\Sigma(\omega) = S(S+1) \frac{\tilde{J}^2}{4z^2} G_{d1}(\omega) \quad (14)$$

where $S=1/2$. The Green's function of dot 1 after including self-energy and vertex correction is given by¹⁶

$$G_{d1}^J(\omega) = \frac{z}{zG_{d1}^{-1}(\omega) - \frac{\tilde{J}^2(\omega)S(S+1)}{4z} G_{d1}(\omega)}, \quad (15)$$

where $\tilde{J}(\omega)$ is replaced by $\gamma(\omega)/\hat{\varrho}(\omega)$, and $G_{d1}(\omega)$ is given by either Eq. (5) (the Dyson equation approach) or Eq. (6) (the single Lorentzian approximation). Note that due to the logarithmic corrections in γ , the spectral density of dot 1 develops a dip at energies $\omega \sim T^* \ll T_K$ for any infinitesimal J , which suppresses the low-energy transmission coefficient through dot 1. Physically, this comes from as a consequence of the fact that electrons of energy $\omega < T^*$ are not energetic enough to break up the local spin singlet and therefore their transport is suppressed. For a finite AF spin-exchange coupling $J > 0$, the real and imaginary parts of $G_{d1}^J(\omega)$ obtained in Eq. (15) via perturbative RG approach lead to an analytical expression for the correction to the LDOS on dot 1, $\delta\rho_c^J(\omega)$,

$$\delta\rho_c^J(\omega) = -\Gamma\rho_0[(q_c^2 - 1)\text{Im } G_{d1}^J(\omega) - 2q_c \text{Re } G_{d1}^J(\omega)]. \quad (16)$$

Below we present the results via NRG with fits by the perturbative RG calculations.

IV. COMPARISON TO THE NRG ANALYSIS

We have performed the NRG calculations on the system in the presence of particle-hole symmetry. The NRG parameters we used are $U_1=U_2=D_0=1$, $\epsilon_{d1}=\epsilon_{d2}=-0.5$, $\Lambda=2$, and $\Gamma_L=\Gamma_R=0.1$ with D_0 being the bandwidth of the conduction-electron baths. (Here, we set $D_0=1$ as the unit of all parameters.) Within each NRG iteration, we keep the lowest 1000 states. For $J=0$, we find $T_K \approx 0.005D_0$. As AF spin-exchange coupling is increased, both real and imaginary parts of $G_{d1}(\omega)$ get splitted at $\omega=0$. First, as shown in Ref. 16, the imaginary part of $G_{d1}(\omega)$ (proportional to DOS of dot 1) at finite J shows a dip below the characteristic energy scale T^* for any arbitrary $J > 0$ [see Fig. 1(a)]. For small AF spin-exchange coupling J , the NRG results for $\text{Im } G_{d1}(\omega)$ can be fitted reasonably well by the perturbative RG approach over an intermediate energy range $T^* \ll \omega \ll T_K$. Furthermore, a clear universal scaling behavior of the Kosterlitz-Thouless (KT) type is observed from the NRG results of $\text{Im } G_{d1}(\omega)$ for $\omega \leq T^*$: $\text{Im } G_{d1}(\omega) \approx g_0 g(\omega/T^*)$ [see Fig. 1(b)].¹⁶ With particle-hole symmetry, the scaling function $g(\omega/T^*)$ is completely universal. As pointed out in Ref. 16, the ground state of the system at any finite J is a local spin singlet (a Fermi

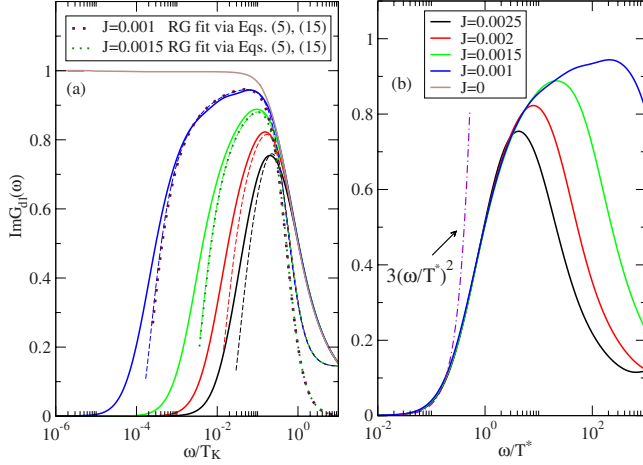


FIG. 1. (Color online) (a) $\text{Im} G_{d1}(\omega)$ [normalized to $\text{Im} G_{d1}(\omega=0, J=0) \approx -1/\Gamma$] of dot 1 with particle-hole symmetry for different AF spin-exchange couplings J calculated by NRG (solid lines) and perturbative RG (dashed lines) via Eqs. (6) and (15) (dashed lines). Dotted lines are RG fits via Eqs. (5) and (15). The NRG parameters are $U_1=U_2=D_0$, $\epsilon_{d1}=\epsilon_{d2}=-0.5D_0$, and $\Gamma=0.2D_0$ with $D_0=1$. For $J=0$, we find $T_K \approx 0.005D_0$. The fitting parameters $c \approx 0.5$ and $\tilde{J} \approx 1.1$. (b) $\text{Im} G_{d1}(\omega/T^*)$ [normalized to $\text{Im} G_{d1}(\omega=0, J=0) \approx -1/\Gamma$] shows a universal scaling behavior for $\omega < T^*$. The dotted-dashed line is the power-law $(\omega/T^*)^{-2}$ fit to the crossover function of $\text{Im} G_{d1}(\omega/T^*)$ for $\omega \ll T^*$, see Eq. (17).

liquid), the very low-energy crossover of $\text{Im} G_{d1}(\omega)$ for $\omega \ll T_K$ vanishes as $(\omega/T^*)^2$, following the Fermi-liquid behavior:

$$-\Gamma \text{Im} G_{d1}(\omega) \approx a_1 \left(\frac{\omega}{T^*} \right)^2, \quad (17)$$

where $a_1 \approx 3.0$ from the fit to the NRG data [see Fig. 1(b)].¹⁶ Note that we find the perturbative RG approach via Eq. (6) leads to a better fit to the NRG results for $\text{Im} G_{d1}(\omega)$ than that via Eq. (5), as expected.

We now discuss the real part of $G_{d1}(\omega)$. For $J=0$, $\text{Re} G_{d1}(\omega)$ is antisymmetric with respect to $\omega=0$ and it shows a peak/dip at $\omega \approx \pm T_K$, signature of the first Kondo effect. As the AF spin-exchange coupling J is increased, the magnitude of the peak/dip in $\text{Re} G_{d1}(\omega)$ for $\omega \approx T_K$ decreases, indicating the Kondo effect is suppressed. At a much lower energy scale, $T^* \approx \omega \ll T_K$, the Kondo dip-peak structure in $\text{Re} G_{d1}(\omega)$ gets a further split with a width $D \approx 2T^*$: it develops a negative-valued dip for $\omega \approx T^*$ while it shows a positive-valued peak for $\omega \approx -T^*$. In the $\omega \rightarrow 0$ limit, both positive and negative branches of $\text{Re} G_{d1}(\omega)$ vanish (see Figs. 2 and 3). We can get an analytical understanding of this behavior as follows: in the Kondo regime $\omega \ll T_K$, the real part of $G_{d1}^J(\omega)$ is approximately given by [see Eq. (15)]

$$\text{Re} G_{d1}^J(\omega) \approx \frac{z\omega \left(1 - \frac{3\tilde{J}^2(\omega)}{16\tilde{T}_K^2} \right)}{\omega^2 \left(1 - \frac{3\tilde{J}^2(\omega)}{16\tilde{T}_K^2} \right)^2 + \tilde{T}_K^2 \left(1 - \frac{3\tilde{J}^2(\omega)}{16\tilde{T}_K^2} \right)^2}. \quad (18)$$

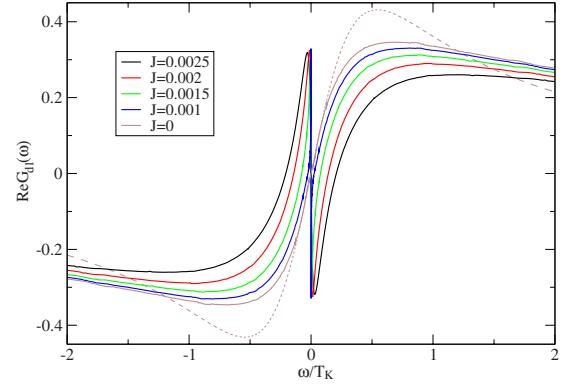


FIG. 2. (Color online) $\text{Re} G_{d1}(\omega)$ [normalized to $-\text{Im} G_{d1}(\omega=0, J=0)$] of dot 1 for different antiferromagnetic spin-exchange couplings J by NRG (solid lines). The dashed line is a fit to the NRG data for $J=0$ via Eq. (6). The other parameters are the same as in Fig. 1.

From the perturbative RG results, as $\omega \rightarrow T^*$, $\tilde{J}(\omega)$ diverges, leading to the vanishing LDOS. As ω decreases to T^* from above, the factor $1 - \frac{3\tilde{J}^2(\omega)}{16\tilde{T}_K^2}$ in Eq. (18) first becomes negative then it approaches 0 as ω further approaches 0. This explains the additional dip-peak structure seen for $|\omega| \rightarrow T^*$ in the NRG results. This qualitative feature can be captured by the perturbative RG approach. However, the magnitudes of the dip-peak features via perturbative RG are much smaller than those obtained from NRG. We believe the reasons for the deviation are twofolds: first, the overall shape of $\text{Re} G_{d1}(\omega)$ predicted via RG is shifted toward the smaller $|\omega|$ region compared to the NRG results. This leads to a smaller value for $\omega_0 > 0$ (compared to that via NRG) where $\text{Re} G_{d1}(|\omega| < \omega_0)$ changes its sign from positive (negative) to negative (positive) for $0 < \omega < \omega_0$ ($-\omega_0 < \omega < 0$). This makes the magnitudes of these additional dips and peaks smaller as

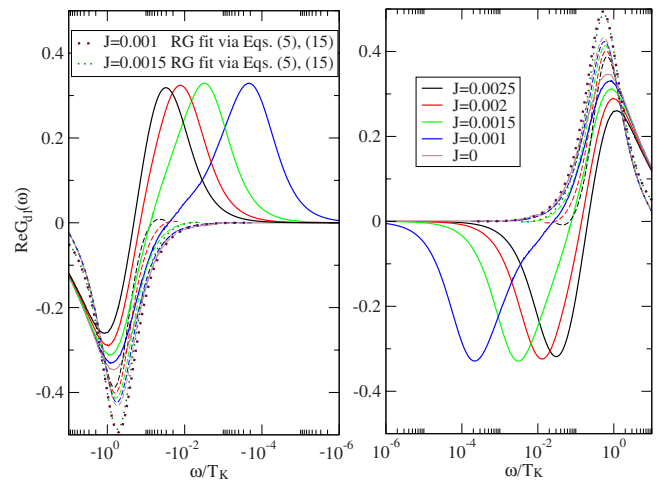


FIG. 3. (Color online) $\text{Re} G_{d1}(\omega)$ [normalized to $-\text{Im} G_{d1}(\omega=0, J=0)$] on a logarithmic scale of ω/T_K for different antiferromagnetic spin-exchange couplings J by NRG (solid lines) and perturbative RG via Eqs. (6) and (15) (dashed lines). Dotted lines are RG fits via Eqs. (5) and (15). The other parameters are the same as in Fig. 1.

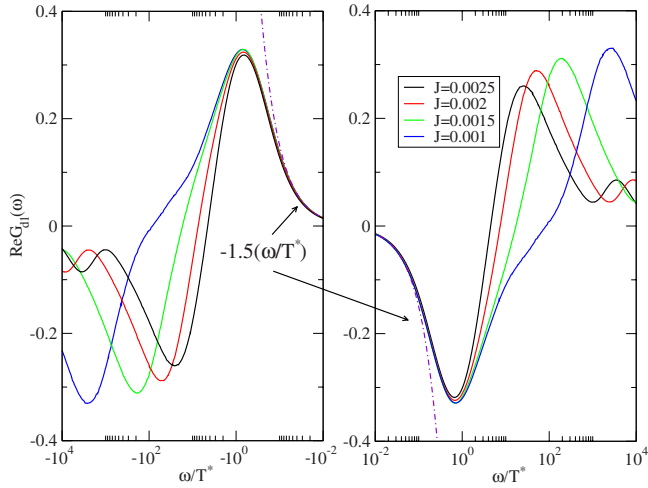


FIG. 4. (Color online) $\text{Re } G_{d1}(\omega)$ [normalized to $-\text{Im } G_{d1}(\omega=0, J=0)$] on a logarithmic scale of ω/T^* for different antiferromagnetic spin-exchange couplings J by NRG. The other parameters are the same as in Fig. 1. The dotted-dashed lines are power-law (ω/T^*) fits to the universal crossover function of $\text{Re } G_{d1}(\omega)$ for $\omega \ll T^*$, see Eq. (19).

$\tilde{J}(\omega)$ diverges even further [see Eq. (18)]. As J is further increased, the deviations between RG and NRG become more transparent. This is expected as the perturbation theory becomes uncontrolled once the system moves away from the weak-coupling regime. Nevertheless, the perturbative RG approach can still capture the qualitative features of $\text{Re } G_{d1}(\omega)$ for $T^* < |\omega| < T_K$ (see Figs. 2 and 3). Note that the perturbative RG approach via Eq. (6) (the Dyson's equation) can fit the NRG result for $\text{Re } G_{d1}(\omega)$ better than that via Eq. (5) for $\omega \geq T_K$, as expected. Similar to the KT scaling behavior for $\text{Im } G_{d1}(\omega)$, the NRG results for $\text{Re } G_{d1}(\omega)$ also show a scaling behavior for $\omega \leq T^*$: $\text{Re } G_{d1}(\omega) \approx g_0' g'(\omega/T^*)$ (see Fig. 4). Here, the scaling function $g'(\omega/T^*)$ is again completely universal in the case of particle-hole symmetry. Based on the Fermi-liquid theory, the very low-energy ($\omega \ll T^*$) crossover function for $\text{Re } G_{d1}(\omega)$ is linear in ω/T^* [see, for example, Eq. (9)],

$$\Gamma \text{Re } G_{d1}(\omega) \approx -a_2 \left(\frac{\omega}{T^*} \right), \quad (19)$$

where we find $a_2 \approx 1.5$ from the fit to the NRG result (see Fig. 4).

Finally, we discuss the behavior for the Fano line shape for $\rho_c(\omega)$. As indicated in Eq. (16), the Fano line shape for $\delta\rho_c(\omega)$ is effectively a linear combination of the asymmetric real part and symmetric imaginary part of the $G_{d1}(\omega)$. The parameter q_c in Eq. (16) depends on the conduction-electron reservoir. Following Refs. 3 and 4, q_c can be reasonably treated as a constant. We take a realistic value $q_c \approx 1.4$ here, corresponding to the Co/Au system studied in Refs. 3 and 7. We find $\rho_c(\omega)$ is asymmetric with respect to $\omega=0$ with a larger magnitude for $\omega > 0$ than that for $\omega < 0$. As shown in Figs. 6 and 7, $\rho_c(\omega)$ shows a dips at $\omega \approx -T_K$ and $\omega \approx T^*$ as well as peaks at $\omega \approx T_K$ and $\omega \approx -T^*$. The peak (dip) at $\omega \approx \pm T_K$ correspond to the first stage Kondo effect while the

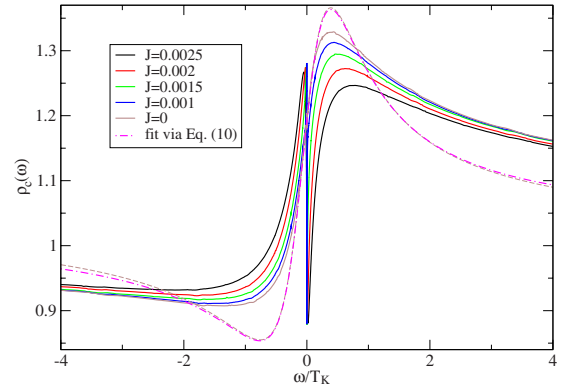


FIG. 5. (Color online) The Fano line shape for $\rho_c(\omega)$ (in unit of ρ_0) for different antiferromagnetic spin-exchange couplings J by NRG. The dashed line is a fit to the Fano line shape forms Eq. (10) for $J=0$. The other parameters are the same as in Fig. 1.

dip (peak) at $\omega \approx \pm T^*$ correspond to the second stage Kondo effect via spin-exchange coupling. We find a reasonably good agreement between the NRG results and the fit via the perturbative RG approach for $T_K \approx \omega < T^*$. [The fit via Eq. (6) is somewhat better than that via Eq. (5) as the former gives a better fit to the NRG result for $\text{Re } G_{d1}(\omega)$.] The above dip-peak structure in the Fano line shape for $\rho_c(\omega)$ in the presence of AF spin-exchange coupling can be detected in the STM measurement of the conduction-electron leads as the signature of the two-stage Kondo effect in side-coupled double quantum dot. Note that the ω/T^* scaling in the NRG results for $\rho_c(\omega)$ is observed (see Figs. 5 and 6), which comes naturally from the scaling behaviors for both real and imaginary parts of $G_{d1}(\omega)$ [see Eq. (3) and Fig. 7]. In the low-energy limit $\omega \ll T^*$ where the system approaches to the Fermi liquid of local spin singlet, we have the following approximated power-law scaling behavior for $\delta\rho_c(\omega)$:

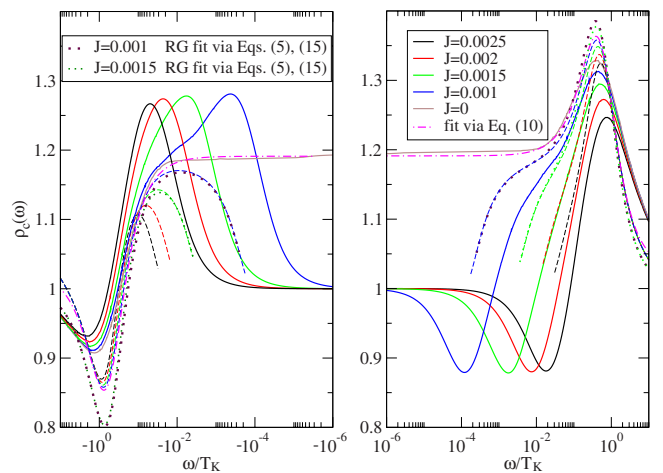


FIG. 6. (Color online) The Fano line shape for $\rho_c(\omega)$ on a logarithmic scale of ω/T_K for different antiferromagnetic spin-exchange couplings J by NRG (solid lines) and perturbative RG via Eqs. (6) and (15) (dashed lines). The dotted-dashed lines are fits to the Fano line shape form via Eq. (10) for $J=0$. The dotted lines are the RG fits via Eqs. (5) and (15). The other parameters are the same as in Fig. 1.

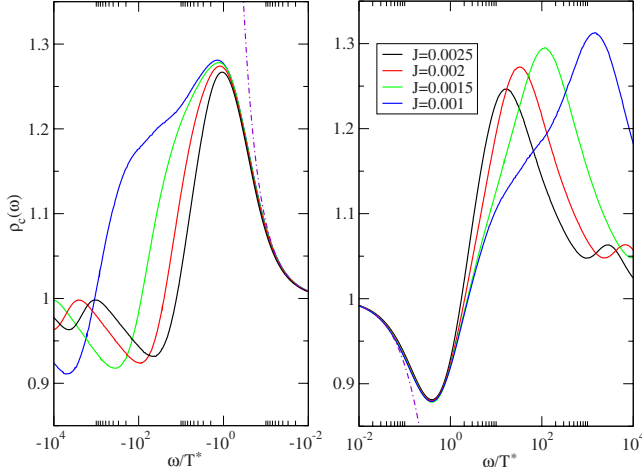


FIG. 7. (Color online) The Fano line shape for $\rho_c(\omega)$ (in unit of ρ_0) on a logarithmic scale of ω/T^* for different antiferromagnetic spin-exchange couplings J by NRG. The other parameters are the same as in Fig. 1. The dotted-dashed lines are power-law fits to the universal scaling function of ω/T^* via Eq. (20).

$$\frac{\delta\rho_c(\omega)}{\rho_0} \approx - \left[(1 - q_c^2) a_1 \left(\frac{\omega}{T^*} \right)^2 + 2a_2 q_c \frac{\omega}{T^*} \right]. \quad (20)$$

For $\omega \ll T_K$, we find the single Lorentzian approximation Eq. (5) can very well describe $G_{d1}(\omega)$; however, for $\omega \leq T_K$, we expect a finite contribution to $G_{d1}(\omega)$ from interference between the Kondo resonance and the broadened impurity level at dot 1. We find indeed a better agreement between the analytic fits and the NRG results for $G_{d1}(\omega)$ and $\rho_c(\omega)$ via perturbative RG approach based on the Dyson's equation Eq. (6) than those from the single Lorentzian fit via Eq. (5).

We would like to make a side remark here. The ‘‘bare’’ resonance width Γ of dot 1 (corresponding to the resonance width of an impurity in a noninteracting resonance-level model) is proportional to the bare constant density of states in the leads ρ_0 . Nevertheless, we find the correction in TDOS in the leads $\delta\rho_c(\omega)$, which comes as a result of the Fano-Kondo interference and AF spin-exchange coupling, does not lead to a sizable feedback effect on Γ within our parameter range. We have checked this numerically via NRG as well as analytically via Eqs. (6) and (15) (combined with the fit to NRG data) where these effects in the leads and on the dots have been properly taken into account. Though this correction exists in principle, we found that it is negligible as the resonance width of dot 1 at $\omega = \epsilon_{d1}$ almost remains unchanged before and after the electron-electron interaction $U_1 = 1$ and/or the small AF spin-exchange couplings $J \ll 1$ (in unit of $D_0 = 1$) are introduced. This comes as a result of the fact that the energy of the dot 1, $\epsilon_{d1} = -U_1/2 \ll 0$, lies well below the Fermi level (or the peak/dip associated with the Kondo effect and AF spin-exchange coupling at energy $\omega \leq T_K$ is well separated from the resonance charge peak of dot 1 with width Γ , $|\epsilon_{d1}| \gg T_K \gg T^*$). Some details are as follows: the bare resonance width of dot 1 is given by (assuming symmetrical hoppings between leads and dot 1: $t = t_L = t_R$) $\Gamma = -1/\text{Im} G_{d1}^0(\omega = \epsilon_{d1}) = 4\pi t^2 \rho_0$. The ratio between the corrected resonance width Γ' and the bare one is given by

$\Gamma'/\Gamma = \frac{1}{\Gamma |\text{Im} G_{d1}^J(\omega = \epsilon_{d1})|}$ [see Eq. (15)]. Since $|\epsilon_{d1}| = U_1/2 \gg T_K \gg T^*$, the frequency-dependent AF spin-exchange coupling is negligible at $\omega = \epsilon_{d1}$, $\tilde{J}(\omega = \epsilon_{d1}) \rightarrow 0$ [see Eq. (12)]. We have therefore $\text{Im} G_{d1}^J(\epsilon_{d1}) \approx \text{Im} G_{d1}(\epsilon_{d1})$. Meanwhile, since the energy of dot 1 is well below the Fermi energy, $\epsilon_{d1} = -U_1/2 \ll 0$ and $|\epsilon_{d1}| \gg T_K$. Via Eq. (6) we have, therefore, $1/\Gamma' = -\text{Im} G_{d1}^J(\epsilon_{d1}) \approx -\text{Im} G_{d1}(\epsilon_{d1}) \approx -\text{Im} G_{d1}^0(\epsilon_{d1}) = 1/\Gamma$. Hence, the correction to Γ is negligible: $\Gamma'/\Gamma \approx 1$.

V. CONCLUSIONS

We have studied the Fano resonance in a side-coupled double quantum dot system in the Kondo regime in the presence of particle-hole symmetry. In the range where the energy of the dot 1 is on the order of the broadening of its energy level, quantum interference between the Kondo effect and the broadened energy level of the dot 1 gives rise to modification of the Green's function on dot 1. We apply the perturbative and numerical renormalization-group approaches to describe the Fano line shape in TDOS of the conduction electrons, which depend on both the real and imaginary parts of the Green's function $G_{d1}(\omega)$ of the dot 1. At $J=0$, $\text{Im} G_{d1}(\omega)$ shows the Kondo peak for $\omega \leq T_K$ while $\text{Re} G_{d1}(\omega)$ exhibits a peak (dip) for $\omega \approx T_K$ ($\omega \approx -T_K$). As a result of the Kondo effect, the Fano line shape in TDOS of the conduction-electron leads shows a peak (dip) around $\omega \approx T_K$ ($\omega \approx -T_K$). At a finite antiferromagnetic spin-exchange coupling between the two dots, the two-stage Kondo effect leads to the suppression of the density of states on dot 1 as well as an additional dip (peak) structure in the real part of $G_{d1}(\omega)$ at $\omega \approx \pm T^*$ from the NRG results. This leads to an additional dip (peak) around $\omega \approx T^*$ ($\omega \approx -T^*$) in the conduction-electron LDOS. The splitting between dip and peak in LDOS at $\omega \approx \pm T^*$ becomes more pronounced as the AF spin-exchange coupling J is increased. At finite values of J and for $\omega < T^*$, the NRG results for $\text{Re} G_{d1}(\omega)$, $\text{Im} G_{d1}(\omega)$, and $\rho_c(\omega)$ all show distinct universal scaling behaviors in ω/T^* . Analytically, we find the perturbative RG approach can qualitatively capture the above behaviors for $T^* \ll \omega \leq T_K$. In particular, compare to the simple Lorentzian approximation for $G_{d1}(\omega)$, we find a better fit to the NRG results for the Fano line shape for $\rho_c(\omega)$ for $T^* \ll \omega \leq T_K$ by taking into account the interference between the Kondo resonance and the broadened impurity level on dot 1 within the Dyson's equation approach. To make contact of our results in the experiments, the asymmetrical double dip/peak structure and the scaling behaviors in the Fano line shape predicted here in the spectral properties of the TDOS of the conduction-electron leads can be detected by the transport through the STM tips⁴ as an indication and direct consequence of the two-stage Kondo effect in our side-coupled double quantum dot system. Finally, we would like to make a remark on the Fano line shape in TDOS of the leads in our system without particle-hole symmetry. In this case, we expect a smooth crossover (instead of the KT type transition) between the Kondo and local singlet phases due to the potential scattering terms generated in the presence of particle-hole asymmetry. Nevertheless, further investigations via NRG are needed to clarify this issue.

ACKNOWLEDGMENTS

We are grateful for the useful discussions with Tao Xiang and P. Wölfle. We also acknowledge the generous support

from the NSC under Grants No. 95-2112-M-009-049-MY3, No. 98-2918-I-009-006, and No. 98-2112-M-009-010-MY3, the MOE-ATU program, the NCTS of Taiwan, R.O.C., and National Center for Theoretical Sciences (NCTS) of Taiwan.

-
- ¹U. Fano, *Phys. Rev.* **124**, 1866 (1961).
²A. C. Hewson, *The Kondo Problem to Heavy Fermions* (Cambridge University Press, Cambridge, UK, 1997).
³H. G. Luo, T. Xiang, X. Q. Wang, Z. B. Su, and L. Yu, *Phys. Rev. Lett.* **92**, 256602 (2004); **96**, 019702 (2006).
⁴O. Újsághy, J. Kroha, L. Szunyogh, and A. Zawadowski, *Phys. Rev. Lett.* **85**, 2557 (2000); Ch. Kolf, J. Kroha, M. Ternes, and W.-D. Schneider, *ibid.* **96**, 019701 (2006).
⁵A. Schiller and S. Hershfield, *Phys. Rev. B* **61**, 9036 (2000).
⁶M. Plihal and J. W. Gadzuk, *Phys. Rev. B* **63**, 085404 (2001).
⁷V. Madhavan, W. Chen, T. Jamneala, M. F. Crommie, and N. S. Wingreen, *Science* **280**, 567 (1998); *Phys. Rev. B* **64**, 165412 (2001).
⁸J. Li, W. D. Schneider, R. Berndt, and B. Delley, *Phys. Rev. Lett.* **80**, 2893 (1998); N. Knorr, M. A. Schneider, L. Diekhoner, P. Wahl, and K. Kern, *ibid.* **88**, 096804 (2002); M. A. Schneider, L. Vitali, N. Knorr, and K. Kern, *Phys. Rev. B* **65**, 121406 (2002).
⁹H. C. Manoharan, C. P. Lutz, and D. M. Eigler, *Nature (London)* **403**, 512 (2000).
¹⁰W. Hofstetter, J. König, and H. Schoeller, *Phys. Rev. Lett.* **87**, 156803 (2001).
¹¹M. Sato, H. Aikawa, K. Kobayashi, S. Katsumoto, and Y. Iye, *Phys. Rev. Lett.* **95**, 066801 (2005).
¹²S. Sasaki, H. Tamura, T. Akazaki, and T. Fujisawa, *Phys. Rev. Lett.* **103**, 266806 (2009).
¹³W.-R. Lee, J. U. Kim, and H.-S. Sim, *Phys. Rev. B* **77**, 033305 (2008).
¹⁴T. Tanamoto, Y. Nishi, and S. Fujita, *J. Phys.: Condens. Matter* **21**, 145501 (2009).
¹⁵A. W. Rushforth, C. G. Smith, I. Farrer, D. A. Ritchie, G. A. C. Jones, D. Anderson, and M. Pepper, *Phys. Rev. B* **73**, 081305(R) (2006).
¹⁶C.-H. Chung, G. Zarand, and P. Wölfle, *Phys. Rev. B* **77**, 035120 (2008).
¹⁷P. S. Cornaglia and D. R. Grempel, *Phys. Rev. B* **71**, 075305 (2005).
¹⁸E. V. Anda, G. Chiappe, C. A. Busser, M. A. Davidovich, G. B. Martins, F. Heidrich-Meisner, and E. Dagotto, *Phys. Rev. B* **78**, 085308 (2008).